UJEAS

UNIZIK JOURNAL OF ENGINEERING AND APPLIED SCIENCES

UNIZIK Journal of Engineering and Applied Sciences 2(3), December 2023, 315-323
Journal homepage: https://journals.unizik.edu.ng/index.php/ujeas
PRINT ISSN: 2992-4383 || ONLINE ISSN: 2992-4391

Empirical Analysis of Ceramic Wear Shrinkage Based on the Operational Influence of Firing Temperature and Sustained Porosity.

C. I. Nwoye[1], C. C. Emekwisia[2*] and C. N. Nwambu[3]
[1,2,3] Chemical Systems and Data Research Laboratory, Department of Metallurgical And Materials Engineering, Nnamdi Azikiwe University Awka, Nigeria.
[*]Corresponding Author's E-mail: cc.emekwisia@unizik.edu.ng

Abstract
The empirical analysis of ceramics ware shrinkage was carried out, based on the operational influence of firing temperature and sustained porosity. This followed derivation of a model expression relating the post-fired volume shrinkage and firing temperature, and sustained porosity. A clay sample was processed following a well detailed step-wise route. The validity of the derived model expressed as; $\xi = 0.15\,\vartheta^2 - 0.953\vartheta + 10^{-6}\text{ɤ} + 21.3$ was rooted in the core expression $\xi - 10^{-6}\text{ɤ} = 0.15\,\vartheta^2 - 0.953\vartheta + 21.3$ where both sides of the expression correspondingly approximately equal. Results generated from both experiment and model prediction indicated that post-fired volume shrinkage increases with decrease in the sustained porosity even when the firing temperature is constant. Evaluated results indicated that the correlations between post-fired volume shrinkage and sustained porosity and the standard error incurred in predicting post-fired volume shrinkage for each value of the sustained porosity considered, as obtained from experiment, derived model and regression model were all > 0.9 as well as 0.0307, 3.21 x 10-5 and 2.24 x 10-5 % respectively. The maximum deviation of the model-predicted post-fired volume shrinkage (from experimental results) was less than 8%.

Keywords: Analysis, ceramic ware shrinkage, porosity, firing temperature**.**

1. Introduction

Research has shown the area of application of clay to include cement production, ceramics, paper-making, foundry, cosmetics, chemical filtering, textiles, and constructions because of its thermal and chemical stability. Milošević and Kaluderović (2017). Clay exists naturally in solids, hydrothermal deposits, sediments, sedimentary rocks, and is found in every state in Nigeria. (Olufemi et al., 2023). Clay minerals regarded as pure clay are majorly white or brightly colored, while the presence of impurities likes a little amount of iron oxide is responsible for the reddish or brownish colors of natural clay. Over the years, different kinds of clay have been characterized, (Lomertwala et al., 2019) and used as good refractory material in the production of glass kilns, hot blast stoves and masonry blast furnaces. The Post-Fired Volume Shrinkage (PFVS) has been predicted (Nwoye, Obidiegwu and Mbah, 2014), based on its apparent porosity (AP) and water absorption capacity (WAC).

This was carried out using a two-factorial empirical model expressed as;

$$Q_1 = -\ 0.3988\,\text{ʃ} - 0.3789\,\xi + 39.256 \qquad (1)$$

Where; ϑ = PFVS, ʃ = AP and ξ = WAC.

The correlations between PFVS and WAC and apparent porosity as obtained from experiment, derived model and regression model were all > 0.97. The maximum deviation of the model-predicted water absorption (from experimental results) was less than 5.57%. This translated into over 94% operational confidence for the derived model as well as over 0.94 effective response coefficients of WAC and apparent porosity to PFVS of the bricks. Although the influence of porosity on the shrinkage of fired clay has been reported (Nwoye, Obidiegwu and Mbah, 2014; Idrees et al., 2023), the vital role played by operational temperature, during clay shrinkage, has raised the need to unravel its

effect on fired clay. Furthermore, firing temperature and clay porosity jointly determine the extent of water evaporation during drying and shrinking of clay undergoing heat-aided processing.

The present work aims at evaluating the ceramic ware shrinkage, based on the operational influence of firing temperature and sustained porosity. This research will be taken further through empirical model derivation to mathematically evaluate the shrinkage of the ceramic ware (when produced), based on the highlighted process parameters. It is strongly believed that the derived model will predict the ware shrinkage within the actual range, on just substituting into the model, values of the operational temperature and sustained clay porosity, providing the boundary conditions are considered.

2.0 Material and methods

The clay sample used was mined near Otamiri river in (Owerri, Imo State). It was dried in the sun for a total of 72 hrs, crushed and sieved to particle sizes: <100μm, 100-300μm, 300-1000μm. In each case 100g of the dried clay was homogenized separately; mixing thoroughly with 10g bentonite (binder) and 6% water (of total weight). It was moulded (in a mould box of dimension length 70mm, width 17mm, and breadth 9mm) and dried at a temperature of 90^{o}C in an electric oven to enhance loss of water by evaporation through a drying time of 1 hr. After the drying process, the moulded materials were fired in a furnace up to a temperature of 1200^{o}C for 12 hrs and allowed to cool in the same furnace for 24 hrs. The bulk density, fractional apparent porosity and water absorbed by the ceramic after firing were evaluated using the standard technique (BS EN ISO 10545-3., 1997). The initial and final length of each sample was measured before and after firing respectively. The values of these lengths were substituted into the conventional formula (BS EN ISO 10545-3., 1997) for calculating fractional volume shrinkage. These values were multiplied by 100 to obtain the percent volume shrinkage.

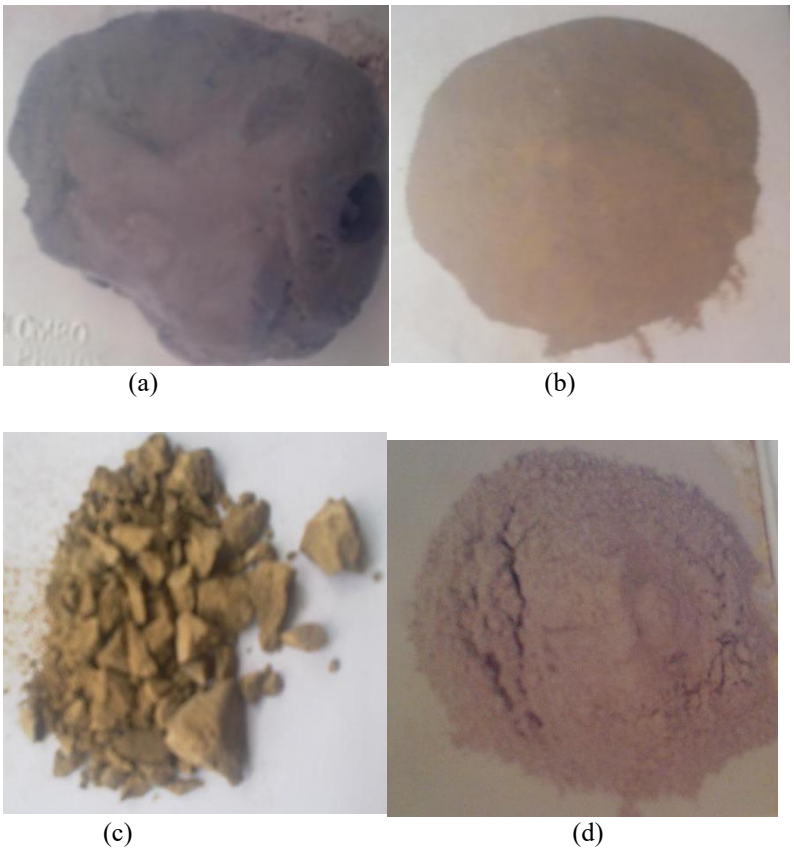

(a) (b)

(c) (d)

Figure 1: (a) Otamiri clay (as mined) (b) Dried and crushed Otamiri clay (c) Dried Otamiri clay mixed with Bentonite (d) Bentonite powder.

Post-fired volume shrinkage V, was calculated using the formular:

$$V = 1 - [(1 - (L - L_3)/L)^3] \times 100 \quad (2)$$

Where;

L = Original length (mm)
L_1 = Dry length (mm)
L_2 = Fired length (mm)

Apparent porosity was determined using the conventional standard technique. [6]

3.0 Results and Discussions

The result of chemical analysis of Otamiri clay is shown in table 1. The table shows that the clay is most constituted by SiO_2 while Na_2O is the poorest constituent.

Table 1: Chemical Composition of Otamiri clays

Constituents	(%)
Al_2O_3	15.60
SiO_2	69.45
TiO_2	1.09
Na_2O	0.01
K_2O	0.21
CaO	0.29
Fe_2O	0.05
LOI	13.10

Table 2: Variation of grain size with post-fired volume shrinkage and sustained fractional porosity

Grain size (µm)	(ɤ)(℃)	(ϑ)	S(%)
(A) <100	1200	0.2559	20.52
(B) 100-300	1200	0.2608	19.93
(C) 300-1000	1200	0.2628	19.63
A + C	1200	0.2593	20.08
A + B	1200	0.2584	20.16

Table 3: Variation of grain size with post-fired volume shrinkage and sustained percent porosity

Grain size (µm)	(ɤ)(℃)	(ϑ)	S(%)
(A) <100	1200	25.59	20.52
(B) 100-300	1200	26.08	19.93
(C) 300-1000	1200	26.28	19.63
A + C	1200	25.93	20.08
A + B	1200	25.84	20.16

Tables 2 and 3 indicate that post-fired volume shrinkage increases with decrease in the sustained porosity, even when the firing temperature was constant. This was so because during firing, water present in the clay was significantly removed, simultaneously accompanied by enhanced decrease in the inter-particle spacing, leading to increased post-fired volume shrinkage. A good knowledge of the empirical relationship between the post-fired shrinkage and firing temperature, and sustained porosity gives a structural engineer an idea of what to expect in terms of cracking or warping of ceramic structures due to over whelming shrinkage resulting from any variation in the firing temperature clay particle size. Table 2 shows that increase in the clay grain size results to decrease in the post-fired shrinkage at

constant firing temperature. This is as a result of increased inter-particle spacing which is likely to retain much water than when the particle size is smaller.

3.1 Model Formulation

Experimental data generated from this research work were used for the model formulation. Computational analysis of the data shown in table 2, gave rise to table 4 which indicate that;

$$\xi - \underline{\mathrm{h}}\gamma \approx K\vartheta^2 - S\vartheta + N \qquad (3)$$

Introducing the values of $\underline{\mathrm{h}}$, N, K and S into equation (3) reduces it to;

$$\xi - 10^{-6}\gamma = 0.15\vartheta^2 - 0.953\vartheta + 21.3 \qquad (4)$$

$$\xi = 0.15\vartheta^2 - 0.953\vartheta + 10^{-6}\gamma + 21.3 \qquad (5)$$

Where

(ξ) = Post fired volume shrinkage (%)

(γ) = Firing temperature (^{o}C)

(ϑ) = Fractional apparent porosity

$\underline{\mathrm{h}} = 10^{-6}$, N = 21.3, K = 0.15 and S = 0.953 These are empirical constants, determined using C-NIKBRAN. (Nwoye, 2008).

3.2 Boundary and Initial Condition

Consider a rectangular shaped clay product of length 49mm, width 17mm, and breadth 9mm exposed to drying in the oven while it was in slight wet condition and then fired in the furnace. Initially, atmospheric levels of oxygen are assumed. Atmospheric pressure was assumed to be acting on the clay samples during the drying process (since the furnace is not air-tight). The sizes of clay particles used were < 100, 100-300 and 300-1000μm while weights of clay and binder (bentonite) used (for each rectangular product) were 100g and 10g respectively. Quantity of water used for mixing was 6% (of total weight). Oven drying and firing temperatures used were 125 and 1200^{o}C for 1and 48 hrs respectively. Area of evaporating surface was 833mm^2. Cooling time for samples was 48 hrs.
The boundary conditions are: atmospheric levels of oxygen at the top and bottom of the clay samples since they are dried under the atmospheric condition. No external force due to compression or tension was applied to the drying clays. The sides of the particles and the rectangular shaped clay products are taken to be symmetries.

3.3 Model Validation

Table 4: Variation of $\xi - 10^{-6}\gamma$ with $0.15\vartheta^2 - 0.953\vartheta + 21.3$

$\xi - 10^{-6}\gamma$	$0.15\vartheta^2 - 0.953\vartheta - 21.3$
20.5188	21.0471
19.9288	21.0413
19.6288	21.0392
20.0788	21.0428
20.1588	21.0437

Equation (5) is the derived model. The validity of the model is strongly rooted on equation (4) where both sides of the equation are correspondingly approximately equal. Table 4 also agrees with equation (4) following the values of $\xi - 10^{-6}\gamma$ and $0.15\vartheta^2 - 0.953\vartheta + 21.3$ evaluated from the experimental results in table 2. Furthermore, the derived model was validated by comparing the derived model-predicted results with standard model-predicted results (regression model-predicted results), carrying out deviational analysis and statistical analysis, involving evaluation of the correlations and standard errors.

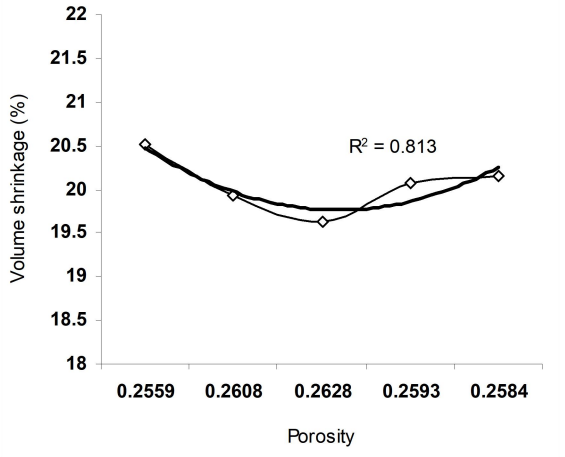

Figure 2: Coefficient of determination between post-fired volume shrinkage and sustained porosity as obtained from experiment.

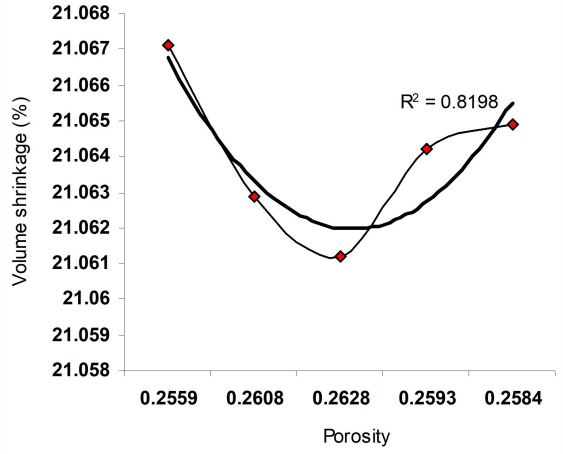

Figure 3: Coefficient of determination between post-fired volume shrinkage and sustained porosity as obtained from derived model.

3.3.1 Statistical Analysis

Standard Error (STEYX)

The standard errors incurred in predicting post-fired shrinkage for each value of the sustained porosity (at constant temperature) considered as obtained from experiment and derived model were 0.0307 and 3.21 x 10^{-5} % respectively. The standard error was evaluated using Microsoft Excel version 2003.

Correlation (CORREL)

The correlation coefficient between post-fired shrinkage and sustained porosity were evaluated from the results of the derived model and experiment, considering the coefficient of determination R^2 from figures 1 and 2. The evaluation was done using Microsoft Excel version 2003.

$$R = \sqrt{R^2} \qquad (6)$$

The evaluated correlations are shown in table 5. These evaluated results indicate that the derived model predictions are significantly reliable and hence valid considering its proximate agreement with results from actual experiment.

Table 5: Comparison of the correlations evaluated from derived model predicted and ExD results based on sustained porosity.

Analysis	Based on sustained porosity	
	ExD	**D-Model**
CORREL	0.9017	0.9054

3.3.2 Graphical Analysis

Comparative graphical analysis of figure 4 shows very close rectangular heights and covered area, representing the experimental (ExD) and model-predicted (MoD) post-fired volume shrinkage.

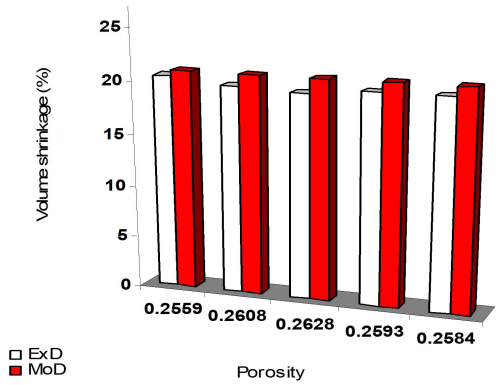

Figure 4: Comparison of post-fired volume shrinkage (relative to sustained fractional porosity) as obtained from experiment and derived model.

Furthermore, the degree of alignment of these curves is indicative of the proximate agreement between both experimental and model-predicted post-fired volume shrinkage.

3.3.3 Comparison of derived model with standard model

The validity of the derived model was also verified through application of the regression model (Reg) in predicting the trend of the experimental results.

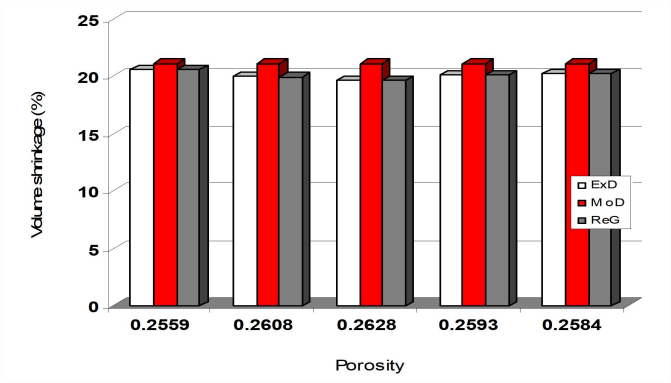

Figure 5: Comparison of post-fired volume shrinkage (relative to sustained fractional porosity) as obtained from experiment, derived model and regression model.

Comparative analysis of figure 5 shows very close rectangular heights and covered area, representing post-fired volume shrinkages. This translated into significantly similar trend of data point's distribution for experimental (ExD), derived model (MoD) and regression model-predicted (ReG) results. Also, the calculated correlations (from figure 5) between post-fired volume shrinkage and sustained porosity for results obtained from regression model gave 0.9088 respectively. These values are in proximate agreement with both experimental and derived model-predicted results. The standard errors incurred in predicting post-fired volume shrinkage for each value of the sustained porosity considered as obtained from regression model was 2.24 x 10^{-5} %.

3.3.4 Deviational Analysis

The deviation Dv, of model-predicted post-fired volume shrinkage from the corresponding experimental result was given by

$$D_v = \left(\frac{\zeta \text{MoD} - \zeta \text{ExD}}{\zeta \text{ExD}}\right) X\ 100 \qquad (7)$$

Where; ζ_{ExD} = Post-fired volume shrinkage obtained from experiment model.

ζ_{MoD} = Post-fired volume shrinkage obtained from derived model.

Critical analysis of the post-fired volume shrinkage obtained from experiment and derived model shows low deviations on the part of the model-predicted values relative to values obtained from the experiment. This was attributed to the fact that the surface properties of clay and the physic-chemical interactions between the clay and the binder which played vital roles during shrinkage were not considered during the model formulation. This necessitated the introduction of correction factor, to bring the model-predicted post-fired volume shrinkage level to those of the corresponding experimental values.

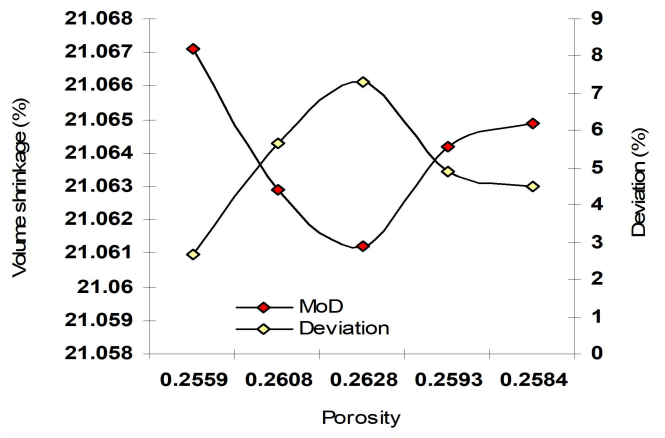

Figure 6: Variation of deviation with post-fired volume shrinkage (relative to sustained fractional porosity).

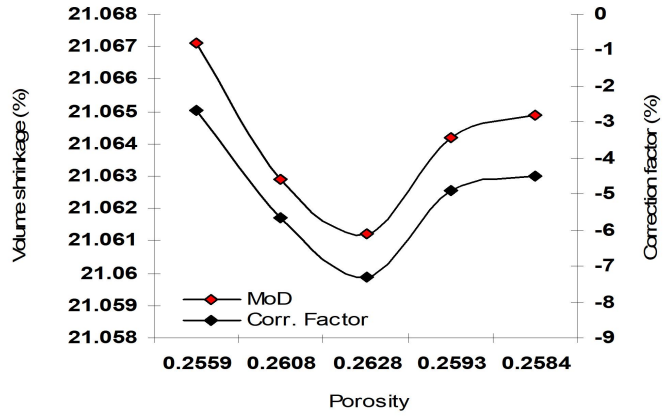

Figure 7: Variation of correction factor with post-fired volume shrinkage (relative to sustained fractional porosity).

Deviational analysis from figure 6 indicates that the maximum deviation of model-predicted post-fired volume shrinkage (from the experimental results) is less than 8%. This translated into over 92% operational confidence for the derived model as well as over 0.92 response coefficients for the dependence of post-fired volume shrinkage of the ceramic on sustained porosity and firing temperature.

Consideration of equation (7) and critical analysis of figure 6 shows that the least and highest magnitudes of deviation of the model-predicted post-fired volume shrinkage (from the corresponding experimental values) are + 2.67 and + 7.29%. figures 3 and 6 indicate that these deviations correspond to post-fired volume shrinkages: 21.0671 and 21.0612 % as well as sustained fractional porosities: 0.2559 and 0.2628 respectively.

Correction factor, Cf to the model-predicted results is given by

$$Cf = -\left(\frac{\zeta \text{MoD} - \zeta \text{ExD}}{\zeta \text{ExD}}\right) X\ 100 \qquad (8)$$

Critical analysis of figures 3, 6 and 7 indicate that the evaluated correction factors are negative of the deviation as shown in equations (7) and (8).

The correction factor took care of the negligence of operational contributions of the surface properties of the clay and the physic-chemical interactions between the clay and the binder which actually played vital role during the shrinkage process. The model predicted results deviated from those of the experiment because these contributions were not considered during the model formulation. Introduction of the corresponding values of Cf from equation (8) into the model gives exactly the corresponding experimental values of post-fired volume shrinkage.

Figure 7 shows that the least and highest correction factor (to the model-predicted post-fired volume shrinkage) are - 2.67 and - 7.29 %. Since correction factor is the negative of deviation as shown in equations (7) and (8), figures 3 and 7 indicate that these highlighted correction factors corresponds to post-fired volume shrinkages: 21.0671 and 21.0612 % as well as sustained fractional porosities: 0.2559 and 0.2628 respectively.
It is very pertinent to state that the deviation of model predicted results from that of the experiment is just the magnitude of the value. The associated sign preceding the value signifies that the deviation is a deficit (negative sign) or surplus (positive sign).

4.0. Conclusion

Empirical analysis of ceramics ware shrinkage was carried out based on operational influence of firing temperature and sustained porosity. This followed derivation of a model expression relating the post-fired volume shrinkage with firing temperature and sustained porosity. The validity of the derived model expressed as; $\xi = 0.159\vartheta^2 - 0.953\vartheta + 10^6\gamma + 21.3$ was rooted in the core expression $\xi - 10^{-6}\gamma = 0.159\vartheta^2 - 0.953\vartheta + 21.3$ where both side of the expression correspondingly approximately equal. Post-fired volume shrinkage increases with decrease in the sustained porosity, even when the firing temperature is constant. Evaluated results indicated that the correlations between post-fired volume shrinkage and sustained porosity and the standard error incurred in predicting post-fired volume shrinkage for each value of the sustained porosity considered, as obtained from experiment, derived model and regression model were all > 0.9 as well as 0.0307, 3.21×10^{-5} and 2.24×10^{-5} % respectively. The maximum deviation of the model-predicted post-fired volume shrinkage (from experimental results) was less than 8%. This translated into over 92% operational confidence for the derived model as well as over 0.92 response coefficients for the dependence of post-fired volume shrinkage of the ceramic ware on the sustained porosity and firing temperature. The derived model will predict the ware shrinkage within the actual range, on substituting into the model, values of the operational temperature and sustained clay porosity, providing the boundary conditions are considered.

References

Milošević, M. M. & Kaluderović, L. J. 2017. Energy Procedia 125, 650–655.

Olufemi, A. O., Francis, K. O., Ogechi, L. A., Kovo, G. A., Anthony, C. O., Helen, O. C., Julius, A., Sunday, C. A., Emmanuel, E. O. 2023. Investigation on the physicochemical properties of Nru clay deposit and its industrial application. Earth Environ. Sci. 1178**,** 012025.

Lomertwala, H. M., Njoroge, P. W., Opiyo, S. A., Ptoton, B. M. 2019. International Journal of Science Research Publication 9, 9581.

Nwoye, C. I., Obidiegwu, E. O., Mbah, C. N., 2014. Production of Bricks for Building Construction and Predictability of Its Post Fired Volume Shrinkage Based on Apparent Porosity and Water Absorption Capacity. Research and Reviews: Journal of Materials Science. 2(3): 17-26.

Idrees, M., Akbar, A., Saeed, F., Gull, M., Eldin, S. M., 2023. Sustainable production of Low-Shrinkage fired clay bricks by utilizing waste plastic dust. Alexandria Engineering Journal 68, 405–416.

BS EN ISO 10545-3: 1997.

Nwoye, C. I. (2008). C-NIKBRAN ‘‘Data Analytical Memory’’- Software.